eLIFE elifesciences.org

RESEARCH ARTICLE

Figures and figure supplements

Filovirus receptor NPC1 contributes to species-specific patterns of ebolavirus susceptibility in bats

Melinda Ng *et al*

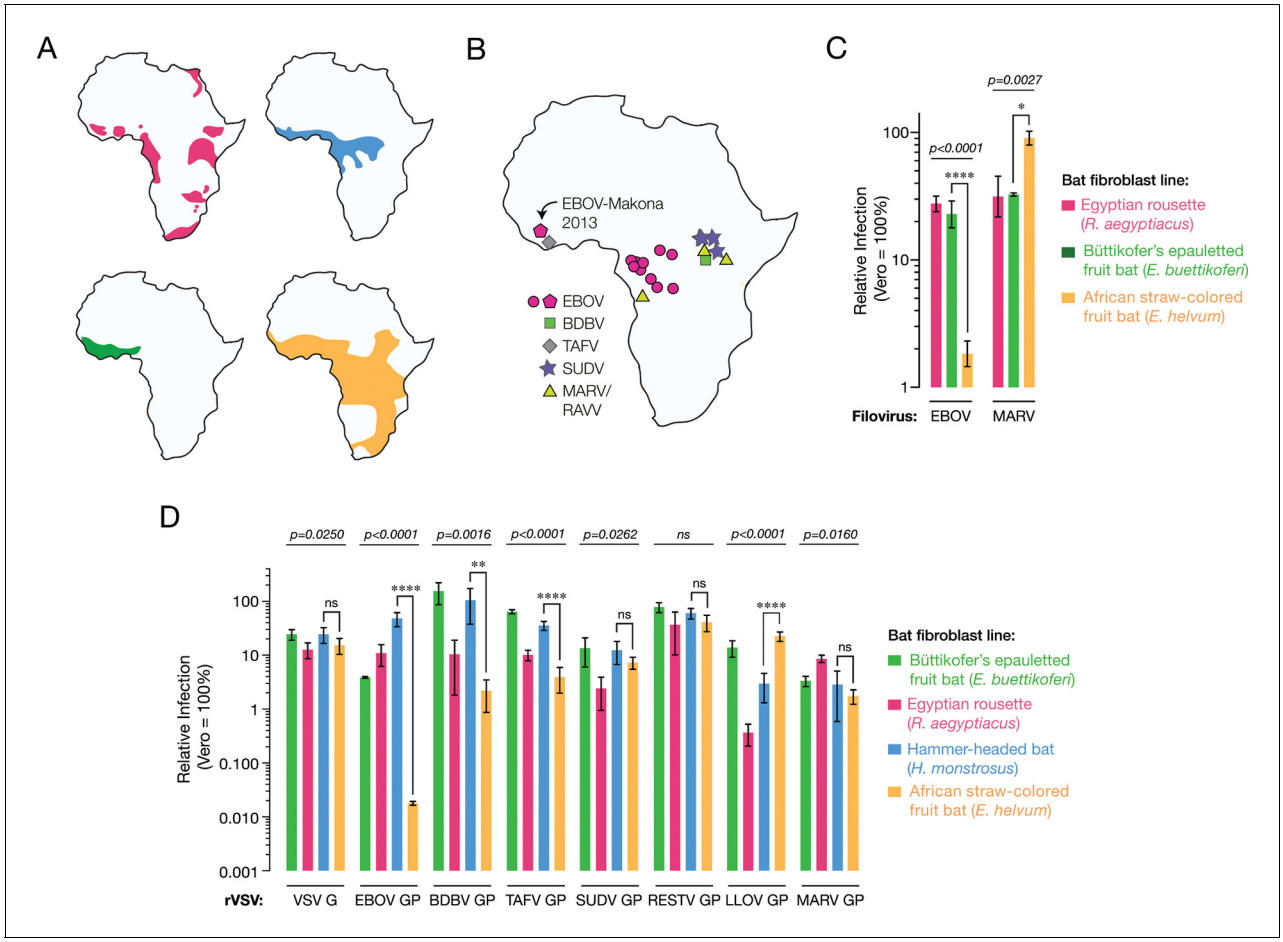

Figure 1. African straw-colored fruit bat cells are refractory to EBOV entry and infection. (**A**) Ranges of African pteropodids *Rousettus aegyptiacus* (pink), *Hypsignathus monstrosus* (blue), *Epomops buettikoferi* (green) and *Eidolon helvum* (yellow) (source: IUCN Redlist). (**B**) Locations of known filovirus outbreaks. (**C**) Infection of pteropodid kidney fibroblast cell lines with authentic filoviruses. Means ± standard deviations ($n \geq 3$) from two biological replicates are shown. (**D**) Infections with recombinant vesicular stomatitis viruses (rVSVs) bearing filovirus glycoproteins. BDBV, Bundibugyo virus; TAFV, Taï Forest virus; SUDV, Sudan virus; RESTV, Reston virus; LLOV, Lloviu virus. Means ± SD ($n = 3–4$) from two biological replicates are shown. In panels C and D, the infectivity of each virus was normalized to that obtained in Vero grivet monkey cells. Means for infection of the different cell lines by each virus were compared by one-way ANOVA (p-value indicated above each group of bars). Tukey's *post hoc* test was used to compare infection means on *Hypsignathus monstrosus* vs *Eidolon helvum* cells (*$p < 0.05$; ****$p < 0.0001$; ns, no statistical significance).

DOI: http://dx.doi.org/10.7554/eLife.11785.003

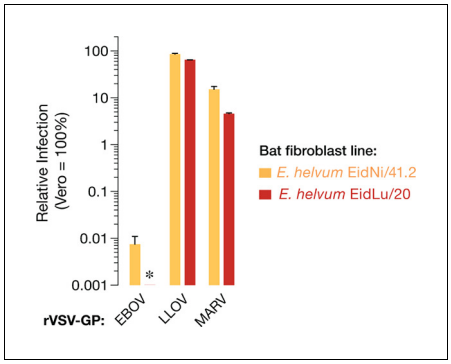

Figure 1—figure supplement 1. Two additional African straw-colored fruit bat cell lines are selectively refractory to EBOV entry and infection. Infection of EidNi/41.2 kidney fibroblasts and EidLu/20 lung fibroblasts with recombinant VSV (rVSVs) bearing filovirus glycoproteins. The infectivity of each virus was normalized to that obtained in Vero grivet monkey cells. Asterisk indicates value below the limit of detection of the infection assay. Means ± SD (n = 4) from two biological replicates are shown.
DOI: http://dx.doi.org/10.7554/eLife.11785.004

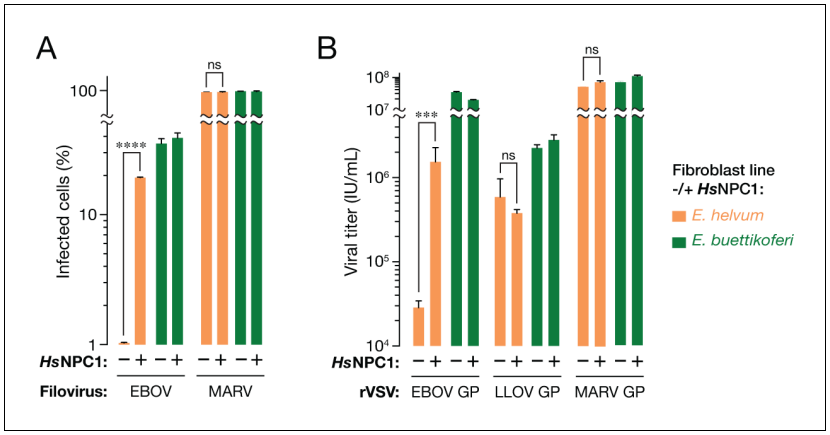

Figure 2. The NPC1-dependent entry and infection block in African straw-colored fruit bat cells is selective for EBOV. (**A**) Infection of pteropodid kidney fibroblast cell lines stably expressing human NPC1 (*Hs*NPC1) with authentic filoviruses. (**B**) Infection of pteropodid kidney fibroblast cell lines with recombinant VSV (rVSVs) bearing filovirus glycoproteins. IU/ml, infectious units per ml. Means ± SD (n = 3) from a representative experiment are shown in each panel. Means for infection of cell lines lacking or ectopically expressing *Hs*NPC1 were compared by unpaired two-tailed Student's t-test with Welch's correction (***p< 0.001; ****p< 0.0001; ns, no statistical significance).

DOI: http://dx.doi.org/10.7554/eLife.11785.005

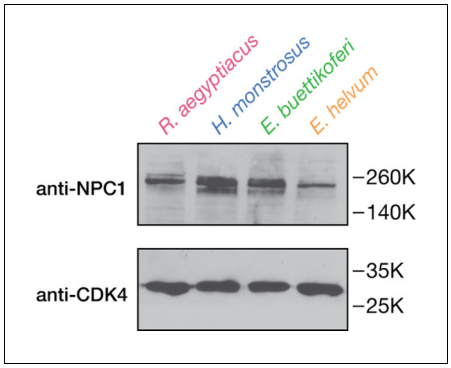

Figure 2—figure supplement 1. Detection of endogenous NPC1 in pteropodid kidney fibroblast cell lines. NPC1 in cell extracts was detected by SDS-PAGE and imunoblotting with an anti-NPC1 antibody specific to the NPC1 cytoplasmic tail. Cyclin-dependent kinase 4 (CDK4) was used as a loading control.
DOI: http://dx.doi.org/10.7554/eLife.11785.006

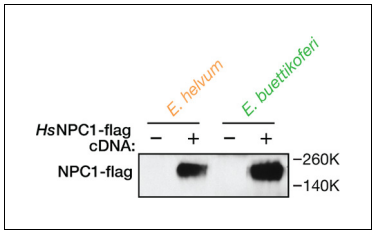

Figure 2—figure supplement 2. Ectopic expression of human NPC1 in pteropodid kidney fibroblast cell lines. Cytoplasmic extracts of pteropodid kidney fibroblast cell lines (control or ectopically expressing flag epitope-tagged human NPC1 [*Hs*NPC1]) were resolved in SDS-polyacrylamide gels and detected by immunoblotting with an anti-flag antibody.
DOI: http://dx.doi.org/10.7554/eLife.11785.007

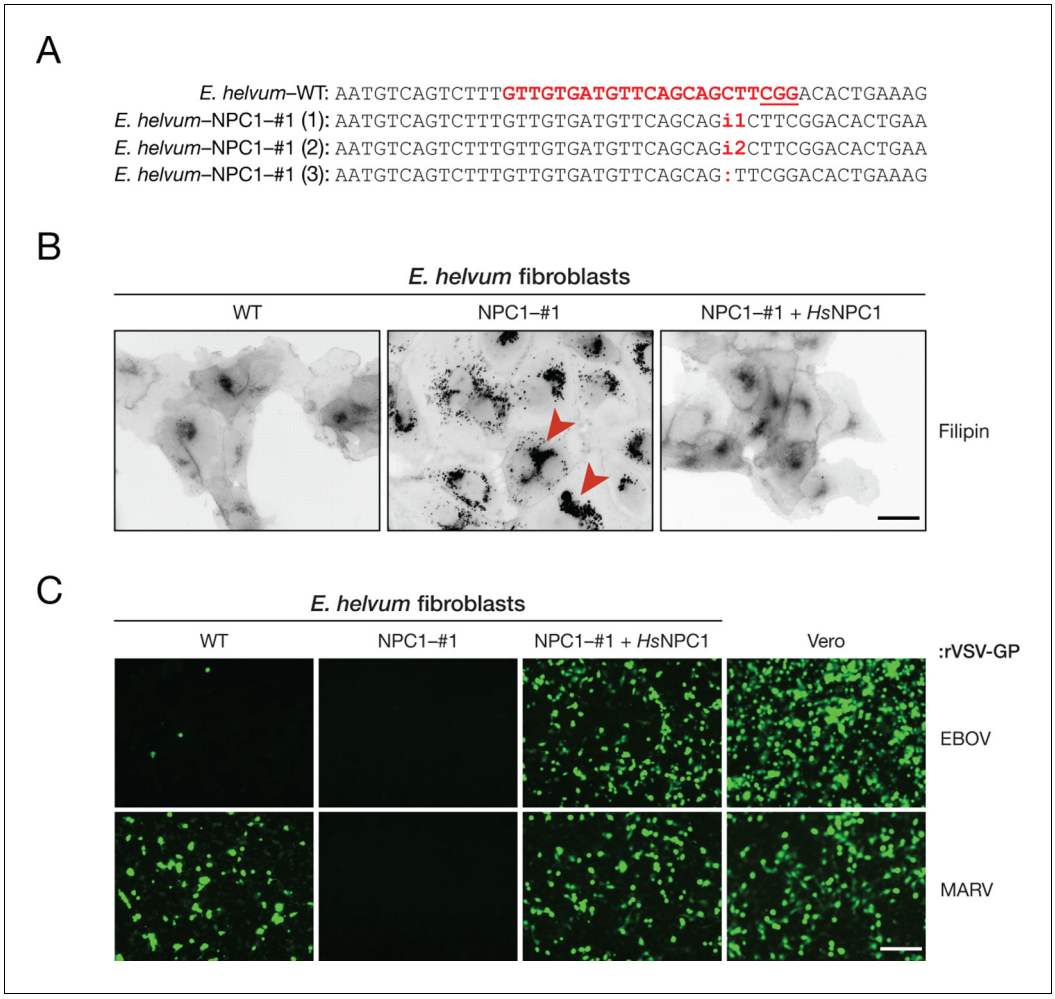

Figure 3. The incompatibility between EBOV GP and *Eidolon helvum* NPC1 reduces, but does not eliminate, EBOV entry into African straw-colored fruit bat cells. (**A**) CRISPR/Cas9 genome engineering was used to knock out the *NPC1* gene in African straw-colored fruit bat kidney fibroblasts. WT *NPC1* gene sequence aligned with the sequences of all three alleles in the knockout (NPC1–#1) cell clone. The gRNA target sequence is marked in red, and the protospacer adjacent motif (PAM) sequence of the gRNA target site is underlined. (**B**) The capacity of WT and NPC1–#1 cells, and NPC1–#1 cells stably expressing *Hs*NPC1, to clear lysosomal cholesterol was determined by staining with filipin III complex from *Streptomyces filipensis*, as described (***Carette et al., 2011***). Red arrowheads indicate lysosomes with accumulated cholesterol. (**C**) Infection of African straw-colored fruit bat cell lines and Vero African grivet monkey cells (control) by VSVs bearing EBOV or MARV GP. Infected (eGFP-positive) cells were visualized by fluorescence microscopy. Representative fields are shown. Scale bars, 20 μm.
DOI: http://dx.doi.org/10.7554/eLife.11785.008

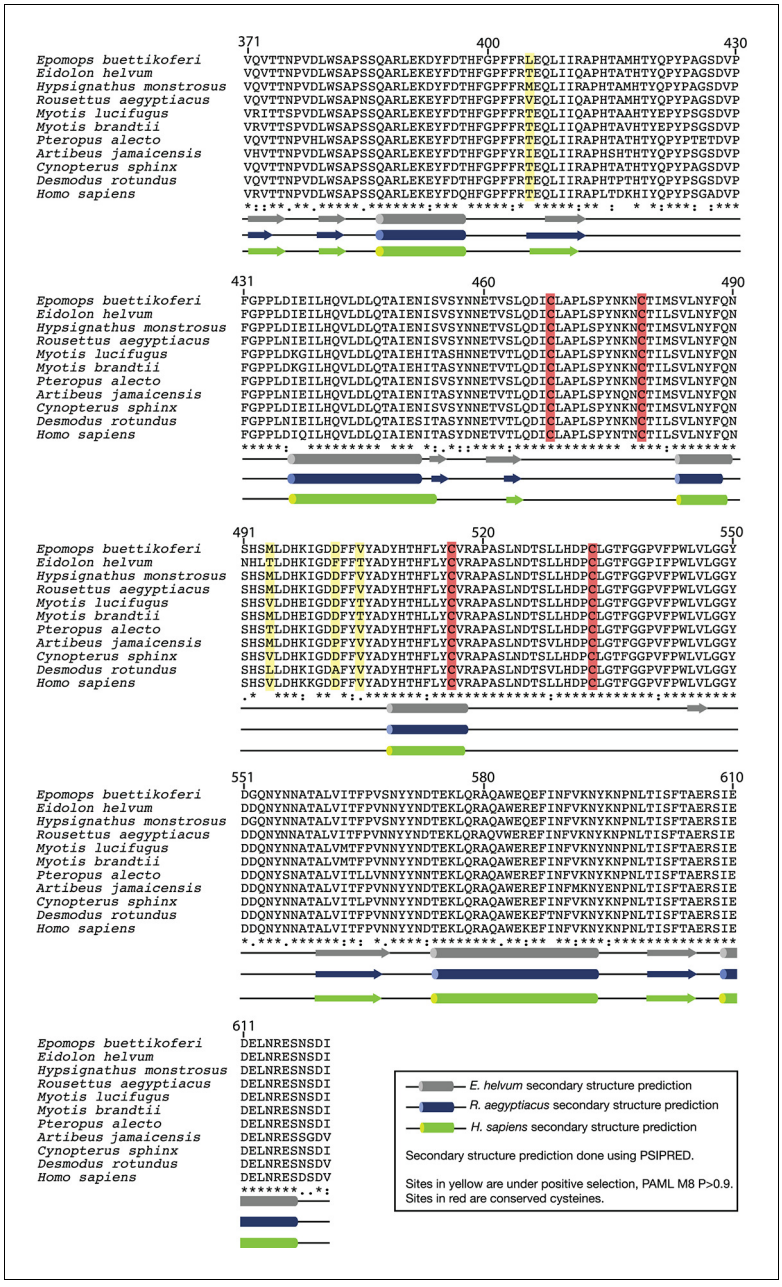

Figure 3—figure supplement 1. Alignment of bat NPC1 domain C amino acid sequences. Conserved cysteine residues are labeled in red.Residues under positive selection (see ***Figure 5***, ***Figure 5—figure supplement 1***, and text) are labeled in yellow. Predicted secondary structures for *H. sapiens, R. aegyptiacus*, and *E. helvum* domain C were generated using PSIPRED and are shown below the alignment.

DOI: http://dx.doi.org/10.7554/eLife.11785.009

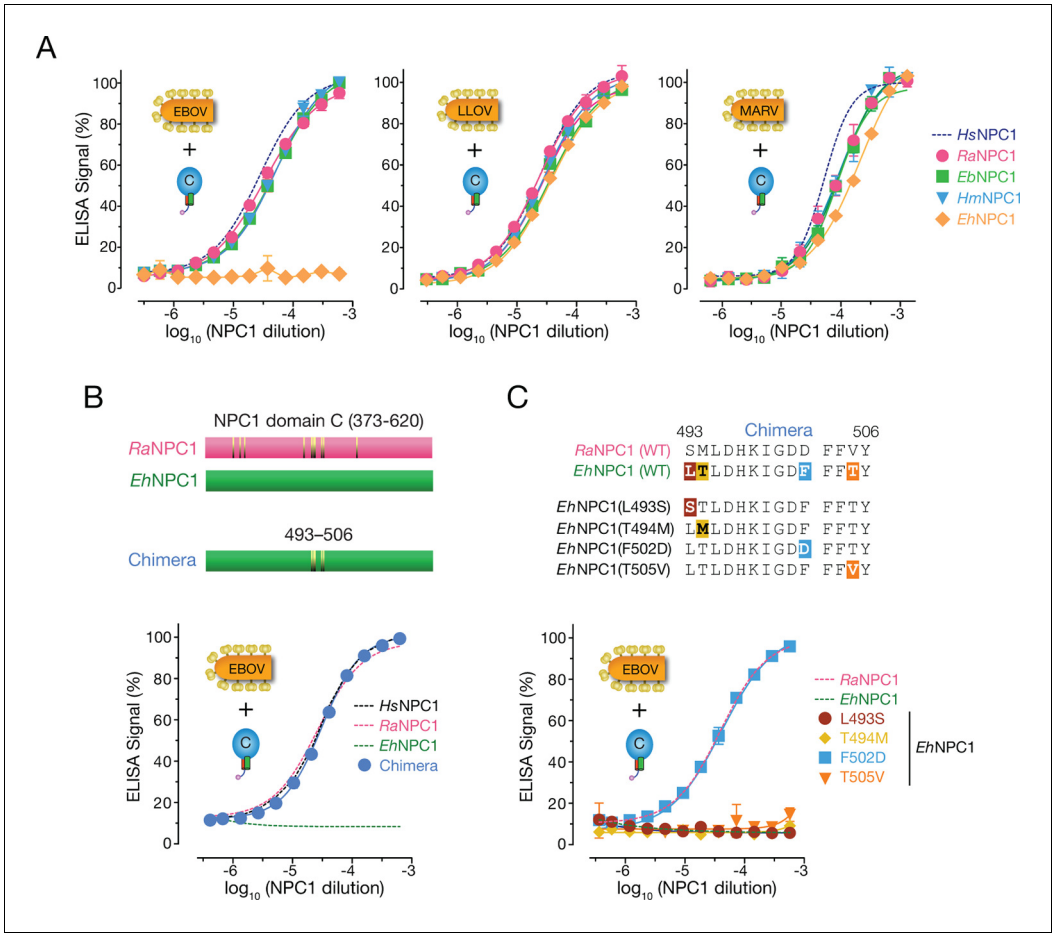

Figure 4. African straw-colored fruit bat NPC1 binds poorly to EBOV GP because of a single amino acid change relative to NPC1 from permissive African pteropodids. (**A**) Binding of filovirus GP proteins to soluble NPC1 domain C proteins derived from African pteropodids measured by an ELISA. *Ra*NPC1, Egyptian rousette; *Eb*NPC1, Büttikofer's epauletted fruit bat; *Hm*NPC1, Hammer-headed bat; *Eh*NPC1, African straw-colored fruit bat. (**B**) A chimera between *Ra*NPC1 and *Eh*NPC1 domain Cs fully rescues EBOV GP-*Eh*NPC1 binding. (**C**) A single amino acid change in *Eh*NPC1 domain C, F502D, renders it fully competent to recognize EBOV GP. Means ± SD (n = 3) from a representative experiment are shown.

DOI: http://dx.doi.org/10.7554/eLife.11785.010

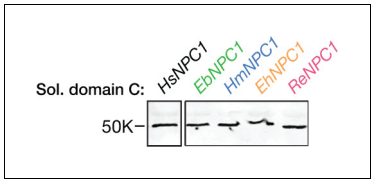

Figure 4—figure supplement 1. Expression of soluble pteropodid NPC1 domain C proteins. Flag epitope-tagged NPC1 domain C proteins derived from pteropodids were expressed in 293T cells, subjected to deglycosylation with protein N–glycosidase F, resolved in SDS-polyacrylamide gels, and detected by immunoblotting with an anti-flag antibody.
DOI: http://dx.doi.org/10.7554/eLife.11785.011

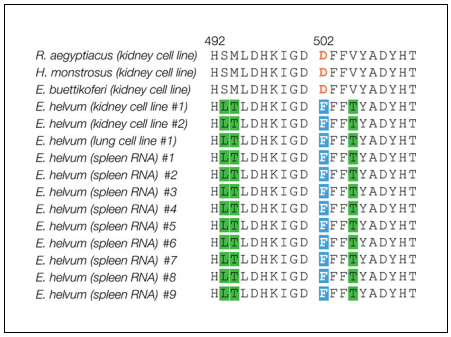

Figure 4—figure supplement 2. Amino acid residue 502 is conserved in NPC1 domain C sequences from additional wild-caught African straw-colored fruit bats. *NPC1* sequences were amplified and sequenced from three African straw-colored fruit bat (*Eidolon helvum*) cell lines and spleen samples derived from nine additional wild-caught *E. helvum* bats. Alignments of domain C amino acid sequences are shown. Residue 502 is highlighted in orange and white text-on-blue shading. Other amino acid changes are highlighted in green.

DOI: http://dx.doi.org/10.7554/eLife.11785.012

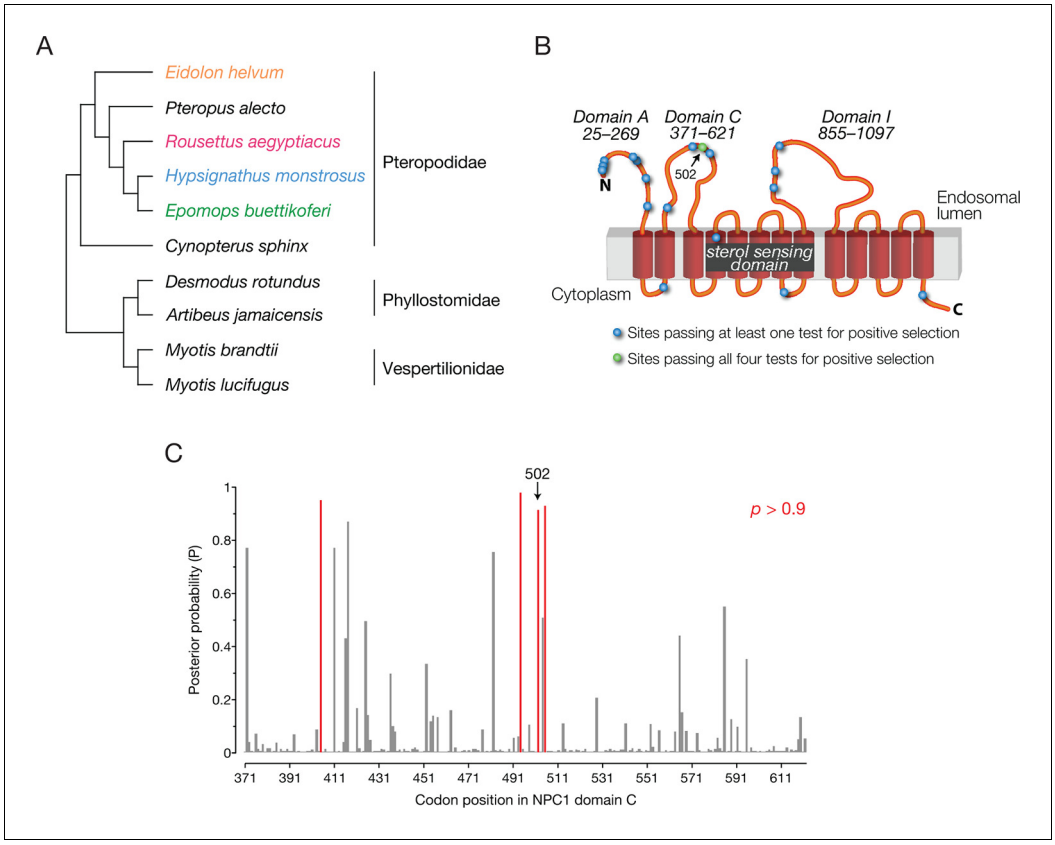

Figure 5. *NPC1* is under positive selection in bats. (**A**) Bat species included in the evolutionary analysis of *NPC1*. Family relationships are indicated at the right of the sequence alignment. (**B**) Positions identified with dN/dS>1 are illustrated on a cartoon schematic of NPC1. Sites in blue were identified in at least one of the four evolutionary analyses performed, and the site in green was identified in all four analyses (***Figure 5—figure supplement 1***). (**C**) The posterior probability that each codon in domain C has dN/dS>1 according to PAML. Position 502 is indicated (p = 0.921), and two clusters of sites with elevated posterior probabilities are evident.

DOI: http://dx.doi.org/10.7554/eLife.11785.013

Species Tree[f]:

PAML M8[a]	FEL[a]	REL[a]	MEME[a]
Codons with dN/dS>1[b] Posterior probability >0.95*, >0.99**	Codons with dN/dS>1[c]	Codons with dN/dS>1[d] BF > 50	Codons with dN/dS>1[e]
47P*, 50P**, 136Q*, 405L*, 494M* **502D (P = 0.921),** 505V, 678A*, 912V, 962S*	**502D (p = 0.051)** 962S (p = 0.055)	6R, 81Q, 86S, 136Q, 214A, 274T, 341Q, **502D (BF =72.631)** 925N, 962S, 1267K	47P (p = 0.01) 49K (p= 0.01) **502D (p= 0.002)**

Gene Tree[f]:

PAML M8[a]	FEL[a]	REL[a]	MEME[a]
Codons with dN/dS>1[b] Posterior probability >0.95*, >0.99**	Codons with dN/dS>1[c]	Codons with dN/dS>1[d] BF > 50	Codons with dN/dS>1[e]
47P*, 49K, 50P**,136Q*, 405L* 417M, 494M*, **502D* (P = 0.957),** 505V*, 678A**, 802R, 903A, 912V*, 962S*	**502D (p = 0.052)** 962S (p = 0.055)	6R, 69G, 81Q, 136Q, 214A, 274T, 341Q, **502D (BF =72.937),** 925N, 962S, 1267K	47P (p = 0.01) 49K (p= 0.01) **502D (p= 0.002)**

[a] Dataset consisted of the aligned *NPC1* from: *E. helvum, H. monstrosus, E. buettikoferi, R. aegyptiacus, P. alecto, C. sphinx, D. rotundus, A. jamaicensis, M. brandtii*, and *M. lucifugus.*

[b] Codons assigned to the dN/dS>1 site class in PAML's M8 model with a posterior probability greater than 0.90 by Naive Empirical Bayes. Residue numbering corresponds to *E. buettikoferi* NPC1.

[c] FEL assigns each codon a rate of synonymous substitution and nonsynonymous substitution. This method determines whether a site is under positive selection by a pairwise comparison (LRT) of a model where dN equals dS and one where dN does not equal dS. Sites less than or near p=0.05 are listed. Residue numbering corresponds to *E.buettikoferi* NPC1.

[d] REL places codons in specific rate classes of dN/dS, similar to PAML. Codons shown are assigned to the dN/dS >1 class with a Bayes Factor greater than 50. Residue numbering corresponds to *E.buettikoferi* NPC1. Residue 6, identified here, is not illustrated or discussed in the manuscript because it is part of a cleaved signal sequence.

[e] Unlike other methods that can only detect sites under pervasive selection, MEME can detect instances of episodic selection. All sites with a significant p-value less than 0.05 are listed. Residue numbering corresponds to *E.buettikoferi* NPC1.

[f] Each analysis was performed with two different trees (below). The gene tree represents the tree derived from *NPC1* sequence information. The species tree represents the currently best-supported relationship of these species found in the literature (Agnarsson et al., 2011, Almeida et al., 2011). These two phylogenies only differ in their placement of *E.helvum* and *P.alecto.*

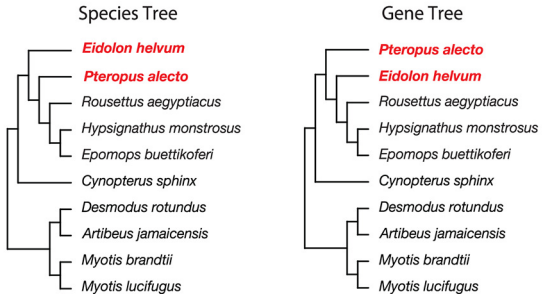

Figure 5—figure supplement 1. Four tests for positive selection in bat *NPC1*. The alignment of bat *NPC1* orthologs was analyzed with four common tests for positive selection (see Materials and Methods for details). Reported in the tables are the codons that were identified by each test to be experiencing positive selection, as described in the footnotes. Two different sets of analyses were performed, one using the species tree (top) and the other using the gene tree (bottom); both trees are shown and contrasted at the bottom.

DOI: http://dx.doi.org/10.7554/eLife.11785.014

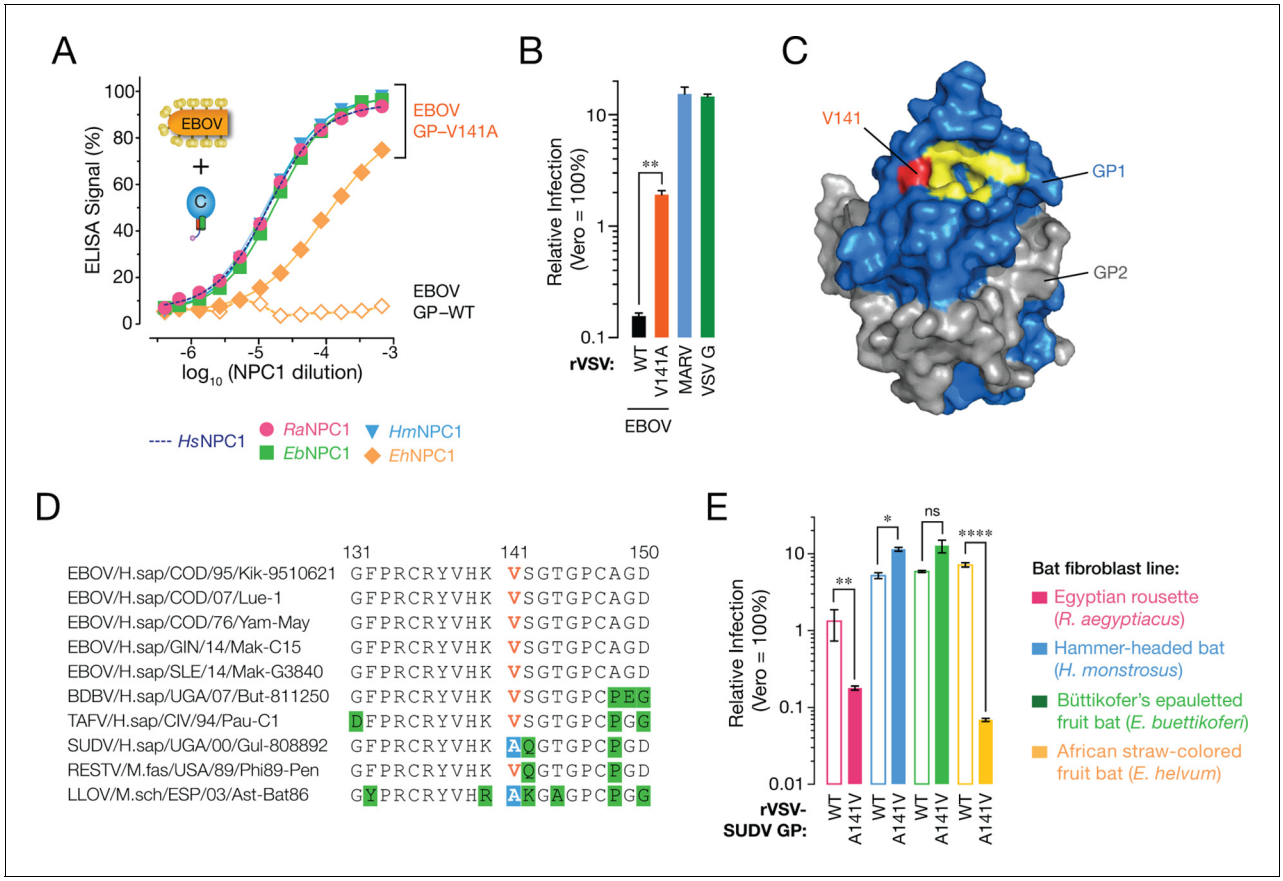

Figure 6. A sequence polymorphism in the NPC1-binding site of filovirus GP influences GP-*Eh*NPC1 binding and *Eh*NPC1-dependent filovirus entry. (**A**) Binding of EBOV GP (WT and mutant V141A) to soluble NPC1 domain C proteins derived from African pteropodids measured by an ELISA. *Ra*NPC1, Egyptian rousette; *Eb*NPC1, Büttikofer's epauletted fruit bat; *Hm*NPC1, Hammer-headed fruit bat; *Eh*NPC1, African straw-colored fruit bat. (**B**) Infection of African straw-colored fruit bat cells with VSV pseudotypes bearing EBOV GP (WT or V141A). Means ± SD (n = 3–4) from a representative experiment are shown in each panel. Means for VSV-EBOV GP WT vs V141A infection were compared by unpaired two-tailed Student's t-test with Welch's correction (**p < 0.01). (**C**) Surface-shaded representation of a single GP1-GP2 monomer (PDB ID: 3CSY (***Lee, et al., 2008***) highlighting key residues in the NPC1-binding site (yellow) and residue 141 (red). GP1, blue. GP2, grey. (**D**) Alignments of GP1 sequences from a panel of filoviruses. V141, orange; A141, white text on blue shading; other residues divergent from consensus sequence, black text on green shading. (**E**) Infection of African pteropodid cells with VSV pseudotypes bearing SUDV GP (WT or A141V). Means ± SD (n = 4) from two biological replicates are shown. Means for VSV-SUDV GP WT vs A141V infection on each cell line were compared by unpaired two-tailed Student's t-test with Welch's correction (*p < 0.05, **p < 0.01, ****p < 0.0001).

DOI: http://dx.doi.org/10.7554/eLife.11785.015

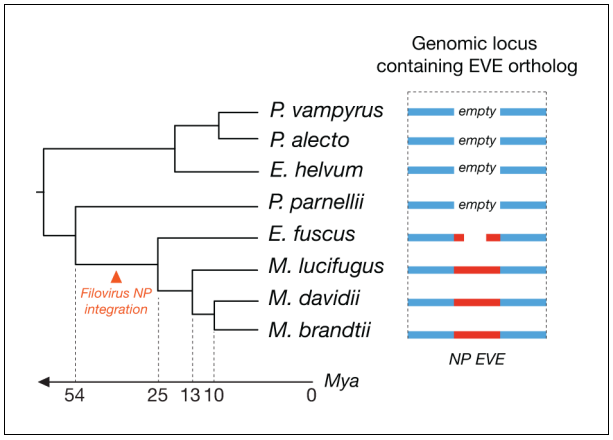

Figure 7. Orthologous endogenous viral elements (EVEs) derived from filovirus nucleoprotein (NP) genes indicate that filoviruses have infected bats for at least 25 million years. The time-calibrated phylogeny shown to the left is based on estimates obtained in ***Miller-Butterworth et al., 2007***. The schematic to the right shows the orthologous EVEs and empty insertion sites as they occur in each bat genome. Also see ***Supplementary file 5***.
DOI: http://dx.doi.org/10.7554/eLife.11785.016